

Short Communication

Vanadium Species in $\text{CH}_3\text{SO}_3\text{H}$ and H_2SO_4 Mixed Acid as the Supporting Electrolyte for Vanadium Redox Flow Battery

Sui Peng¹, Nan-Fang Wang¹, Xiao-Juan Wu¹, Su-Qin Liu^{1,*}, Dong Fang², You-Nian Liu, Ke-Long Huang¹

¹ Institute of Functional Materials, College of Chemistry and Chemical Engineering, Chemistry Building, Central South University, Changsha, Hunan. 410083

² Key Lab of Green Processing and Functional Textiles of New Textile Materials, Ministry of Education, College of Materials Science and Engineering, Wuhan Textile University, 430073, Wuhan, China

*E-mail: sqliu2003@126.com

Received: 26 November 2011 / Accepted: 18 December 2011 / Published: 1 January 2012

Cyclic voltammetry (CV) and electrochemical impedance spectroscopies (EIS) of 2M V(IV) electrolyte in $\text{CH}_3\text{SO}_3\text{H}$ and H_2SO_4 mixed acid solution (MAS sample) and in H_2SO_4 (Pristine sample) as the positive electrolyte in vanadium redox flow battery (VRFB) were investigated. CV results revealed that the MAS sample had a higher reversible redox reaction than Pristine sample. EIS showed that. The performance of a VRFB with MAS sample as positive electrolyte was investigated with the charge-discharge technique. At 120 mA/cm^2 , VRFB with MAS sample exhibited the higher energy density (39.87 Wh/L) in comparison of Pristine sample. Cycling tests indicated that VRFB with the mixed acid system possessed a stable cycling performance during 30 cycles.

Keywords: Vanadium redox flow battery; electrochemical reversibility; Methane sulfonic acid; Energy density; Mixed acid solution

1. INTRODUCTION

Vanadium redox flow battery (VRFB) has higher energy efficiency, longer operation life as well as lower cost compared with other redox batteries. These advantages make the VRB system the most practical candidate for a large-scale energy storage[1-6]. The total amount of energy storage of VRB system is determined by the concentration and volume of the vanadium electrolyte since the negative (V(II)/V(III) redox couple) and positive (V(V)/V(IV) redox couple) electrolytes, the origin of capacity, are stored in reservoirs, respectively. Accordingly, the electrolyte is one of the most

important components for VRFB, which is acted as not only the conductor of the ion but also the energy storage medium. When the volume of the reservoirs for the VRFB system is designed completely, the concentration of vanadium electrolyte could be of importance for improving its energy density.

However, it is very difficult to obtain a higher concentration of vanadium species than 1.8M in sulfuric acid solution due to their limited solubility and stability, especially the V(V) electrolyte, which suffers from thermal precipitation above 40 °C. For the purpose of increasing the solubility and stability of the electrolytes, various strategies has been proposed successively, such as adding organic or inorganic additives [7-10], increasing the concentration of the sulfuric acid and employing a hydrochloric-sulfuric mixed acid [11]. However, the concentration of stable vanadium species could not be exceeded 1.8M. $\text{CH}_3\text{SO}_3\text{H}$ is a much stronger acid than H_2SO_4 and has been well used as supporting electrolyte in other flow batteries [12,13]. To the best of our knowledge, there is no literature describing mixed-acid ($\text{CH}_3\text{SO}_3\text{H}$ and H_2SO_4) electrolyte used in VRFB system.

To increase energy density of VRFB, 2M V(IV) electrolyte in 1.5M $\text{CH}_3\text{SO}_3\text{H}$ and 1.5M H_2SO_4 mixed acid was prepared. Its electrochemical properties were evaluated by cyclic voltammetry (CV) and Electrochemical impedance spectroscopies (EIS). Its performance in VRFB was investigated by charge-discharge technique.

2. EXPERIMENTAL

2.1. CV

2M V(IV) electrolyte in mixed acid (MAS sample) and in H_2SO_4 (Pristine sample) were obtain by dissolving vanadyl sulfate ($\text{VOSO}_4 \cdot n\text{H}_2\text{O}(\text{s})$, Shanghai Huating Chemical Co. Ltd., China, $n = 3.7$) in 1.5 M $\text{CH}_3\text{SO}_3\text{H}$ + 1.5 M H_2SO_4 and in 3.0 M H_2SO_4 , respectively. CV measurements were carried out by using electrochemical workstation (Shanghai Chenhua Instrument Co. Ltd., China) at a scan rate of 10.0-100.0 $\text{mV} \cdot \text{s}^{-1}$ between 0 V and 1.6 V at room temperature. A three-electrode cell was used with Pt piece (1.0 cm^2) as counter electrode, where a saturated calomel electrode (SCE) along with a salt bridge was used as reference electrode and the graphite electrode with a surface area of 1.0 cm^2 was used as working electrode. The graphite electrode was polished with 600 (P1200) grit SiC paper, then washed with de-ionized water as described in the literature [14,15]. To avoid cross-contamination of different ions on the electrodes surface, the graphite electrode was polished and rinsed carefully after each test.

2.2. EIS

EIS was performed with a ZAHNER-IM6 electrochemical workstation (Germany). The sinusoidal excitation voltage applied to the cells was 5 mV with a frequency range from 0.001 Hz to 100 kHz.

2.3. Cell test

A VRFB single cell was fabricated by sandwiching the membrane between two pieces of carbon felt (thickness is 5 cm, Shenhe carbon fiber Materials Co., Ltd.) with effective reaction area of 30 cm², which was served as the electrodes, and conductive plastic were used as the current collectors. 80 mL solutions of 2 M V⁴⁺ in 3.0 M H₂SO₄ serving as negative and 160 mL of MAS sample as positive electrolytes, were cyclically pumped into the corresponding half-cell respectively. The single cell was charged and discharged by a CT2001C-10V/10A battery test system (Wuhan Land Co., Ltd.) with a constant current density of 120 mA/cm². To avoid the corrosion of the carbon felt electrodes and conductive plastic, the upper limit of charge voltage was 1.7 V and the lower limit of discharge voltage was 0.7 V.

3. RESULTS AND DISCUSSION

3.1. CV analysis

The CV curves of for MAS and Pristine samples at 10 mV/s are shown in Fig. 1a.

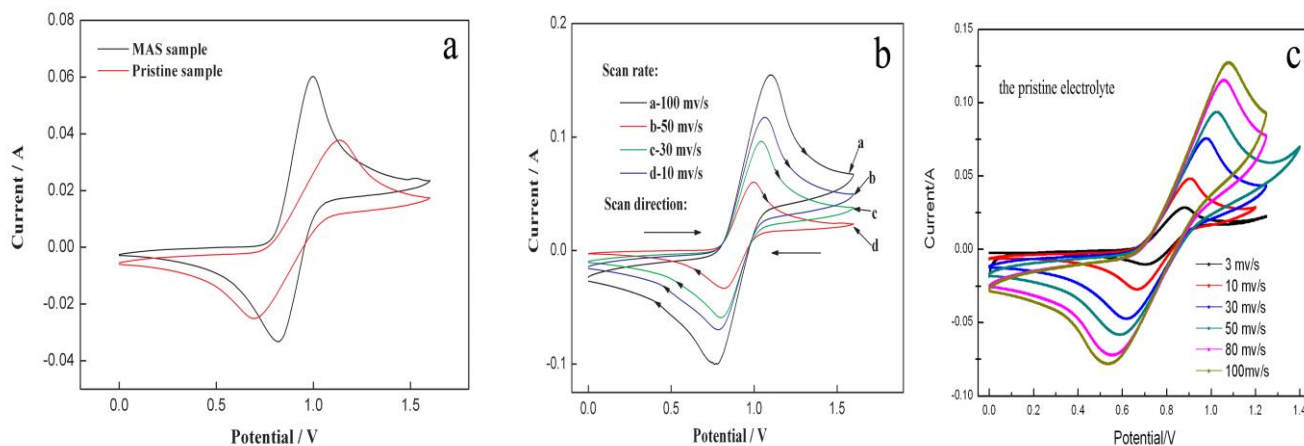


Figure 1. Cyclic voltammograms of MAS and Pristine samples at 25°C: (a) at a scan rate of 10mV/s for MAS and Pristine samples, (b) scan rate from 10 to 100 mV/s for MAS sample, (c) scan rate from 3 to 100 mV/s for Pristine sample.

The reduction peak current of MAS are much higher than that of Pristine, indicating that the V(IV)/ V(V) redox reaction kinetics in mixed acid system is higher than that in single acid system. Furthermore, the difference between oxidation and reduction peak potential (ΔE_p) for MAS is less than that for Pristine, suggesting that V(IV)/V(V) redox reaction in mixed acid system is more electrochemically reversible. Fig. 1b and Fig. 1c show the CVs for V(IV) in MAS and pristine samples at various scanning rates respectively. The peak separation between cathodic and anodic peak (ΔE_p) for MAS sample (Fig. 1b) with the scan rate is slower than that for the pristine sample (Fig. 1c). Plots

of the peak current (i_p) vs. the square root of the scan rate ($v^{1/2}$) is linear, confirming that the oxidation of V(IV) is controlled by mass transport. So the Randles-Sevcik equation could be used to obtain the diffusion coefficient for V(IV) in the MAS and pristine samples. and the calculated values were $8.22 \times 10^{-7} \text{ cm}^2 \text{ s}^{-1}$ and $5.23 \times 10^{-7} \text{ cm}^2 \text{ s}^{-1}$, respectively. These results indicate that V(V)/V(IV) in mixed acid significantly improved the reversibility of the redox as well as the coefficient of mass transport.

3.2. EIS analysis

EIS was further applied to analyze the effect of supporting electrolyte on the performance of the V(IV) electrolyte.

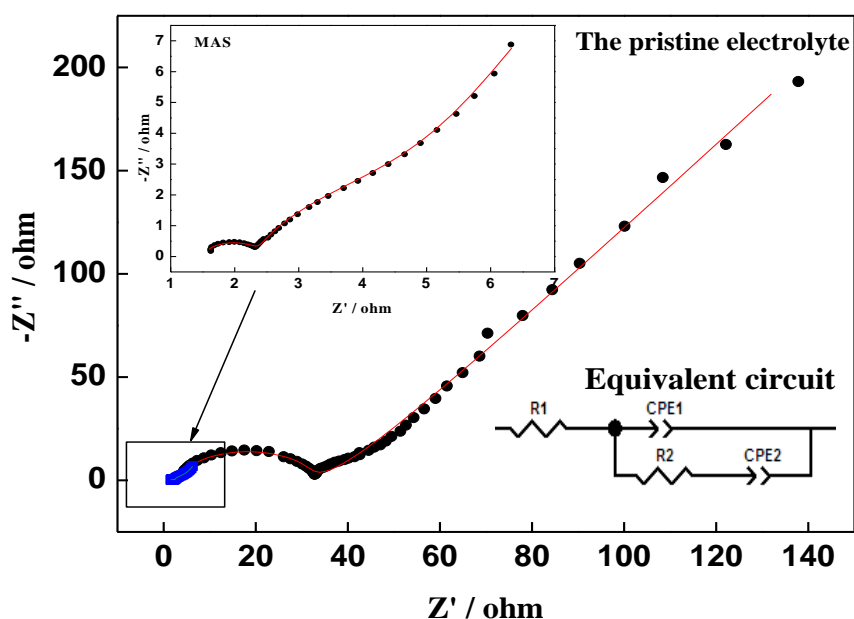


Figure 2. Electrochemical impedance spectroscopy (EIS) of MAS and Pristine samples.

Fig. 2 show the electrochemical impedance spectroscopy (EIS) (Nyquist plots) of MAS and Pristine. Each Nyquist plot includes a semicircle part (the charge transfer process) and a linear part (the diffusion processes) [16-19], indicating that the V(IV)/V(V) redox reaction for MAS and Pristine is mixed-controlled by charge transfer and diffusion steps. Thus, the Nyquist plots can be fitted with the equivalent circuit (Fig. 2). In the equivalent circuit, R_1 stands for the resistance composed of solution resistance (R_s) and (R_e), R_2 represents charge transfer resistance across electrode/solution interface (R_{ct}), CPE_1 is the constant-phase element which represents the electric double-layer capacitance of electrode/solution interface, and CPE_2 is the constant-phase which represents the diffusion capacitance attributed by the diffusion process of V(IV) and V(V) ions in pore channel of the graphite electrodes.[20] Table 1 lists the parameters obtained from fitting the experimental spectroscopy.

Table 1. Fitting results from EIS.

Sample	$(R_1)/\Omega\text{cm}^2$	CPE ₁		$(R_2)/\Omega\text{cm}^2$	CPE ₂	
		$Y_{0.1}$	n_1		$Y_{0.2}$	n_2
Pristine electrolyte	3.558	7.123×10^{-4}	0.9081	28.02	1.162×10^{-7}	0.9718
MAS	1.462	1.781×10^{-3}	0.6154	0.6668	1.392×10^{-6}	0.9982

R1 and R2 of MAS are lower than that of Pristine, implying that the addition of CH₃SO₃H could decrease the solution resistance and facilitate the charge transfer reaction. Additionally, Y01 for MAS is higher compared to Pristine indicating that MAS can enhance diffusion process of V(IV) and V(V) ions in pore channel of the graphite electrodes [21].

3.3. Single cell performance

The discharge capacity and discharge energy decay of VRFB with MAS and Pristine as positive electrolyte respectively at a current density of 120 mA/cm² during charge-discharge cycles are presented in Fig.3.

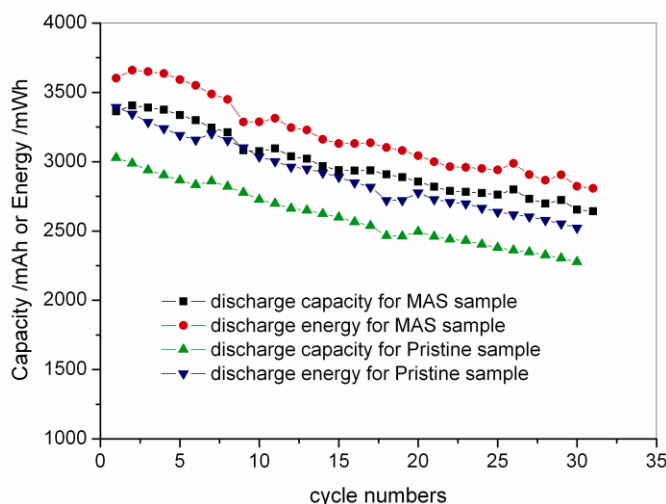


Figure 3. Discharge capacity and energy of VRB with MAS and Pristine samples.

With the cycle increasing, the decay rate of discharge capacity and discharge energy for MAS sample was nearly as same as that for Pristine sample due to the same self discharge rates for the two samples. In the whole charge-discharge cycles, the VRB with MAS exhibits larger discharge capacity and discharge energy than that with Pristine, due to its better reversibility and electrochemical reaction reversibility verified by CV and EIS. The corresponding energy density is 39.87 Wh/L, 36.27 Wh/L, respectively, revealing that CH₃SO₃H as supporting electrolyte can improve the energy density of the VRFB.

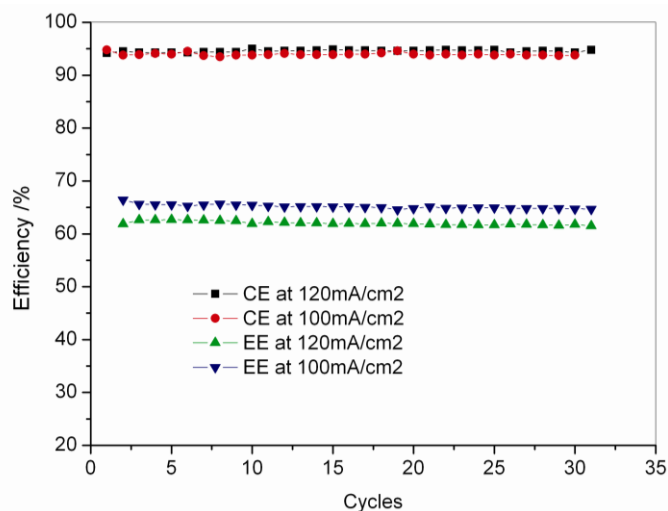


Figure 4. Coulombic efficiency and energy efficiency stability of VRFB with MAS at 100mA/cm² and 120mA/cm²

Fig.4 displays the coulombic efficiency and energy efficiency stability of VRFB with MAS at 100mA/cm² and 120mA/cm², respectively. In 30 cycles, the VRFB with MAS has a stable coulombic efficiency and energy efficiency. Increasing the current density, the coulombic efficiency maintained about 94% while energy efficiency decreased from 65% to 61% due to greater polarisation at higher charge-discharge current density. These results imply the VRB with MAS is applicable for energy reservation.

4. CONCLUSIONS

CV and EIS techniques were used to investigate the electrochemical properties of V(IV) electrolyte with MAS. The results showed the electrochemical activity of the electrolyte with MAS was significantly improved compared with that in sulfuric acid. Compared to sulfuric acid, MAS supporting electrolyte has two main advantages. One is the increasing of redox reaction kinetics between V(IV) and V(V), and the other is the decreasing of mass transport resistance. The VRFB with MAS sample showed much higher energy density of 39.87 Wh/L than that (36.27 Wh/L) for Pristine sample. The cycling data show that the VRFB with MAS system has a good stability.

ACKNOWLEDGEMENTS

This work was financially supported by the Major State Basic Research Development Program of China (973 Program) (No. 2010CB227201), the Natural Science Foundation of China (No, 51072234)

References

1. L. Joerissen, J. Garche, C. Fabjan, G. Tomazic, *J.PowerSources*, 127 (2004) 98
2. P. Zhao, H.M. Zhang, H.T. Zhou, B.L. Yi, *Electrochim. Acta* 51 (2005) 1091

3. C. Fabjan, J. Garche, B. Harrer, L. Jorissen, C. Kolbeck, F. Philippi, G. Tomazic, F. Wagner, *Electrochim. Acta*, 47 (2001) 825
4. K.L. Huang, X.G. Li, S.Q. Liu, N. Tan, L.Q. Chen, *Renewable Energy*, 33(2008) 186
5. C. Ponce De Leon, A. Frias-Ferrer, J. Gonzalez-Garcia, D.A. Szanto, F.C. Walsh, *J Power Sources*, 160 (206) 716
6. K.L. Huang, X.G. Li, S.Q. Liu, N. Tan, L.Q. Chen. *Renewable Energy*, 33 (2008) 186
7. C. Fabjan, J. Garche, B. Harrer, L. Jörissen, C. Kolbeck, F. Philippi, G. Tomazic, F. Wagner, *Electrochimica Acta*, 47 (2001) 825
8. F. Rahman, M. Skyllas-Kazacos, *J. Power Sources*, 72 (1998) 105
9. F. Rahman, M. Skyllas-Kazacos, *J. Power Sources*, 189 (2009) 1212
10. F. Rahman, M. Skyllas-Kazacos, *J. Power Sources*, 189 (2009) 1212
11. N. Kausar, R. Howe, M. Skyllas-Kazacos, *J. Appl. Electrochem.*, 31 (2001) 1327
12. Liyu Li, Soowhan Kim, Wei Wang, M. Vijayakumar, Zimin Nie, Baowei Chen, Jianlu Zhang, Guanguang Xia, Jianzhi Hu, Gordon Graff, Jun Liu, Zhenguo Yang, *Advanced Energy Materials*, 3 (2011) 394
13. Zhipeng Xie, Fengjiao Xiong, Debi Zhou. *Energy Fuels*, 25 (2011) 2399
14. Derek Pletcher, Hantao Zhou, Gareth Kearb, C.T. John Lowb, Frank C. Walshb, Richard G.A. Wills b, *Physical Chemistry Chemical Physics*, 180 (2008) 621
15. Y. Matsuda, K. Tanaka, M. Okada, Y. Takasu, M. Morita, T. Matsumura-Inoue, *J. Appl. Electrochem*, 18 (1988) 909
16. S. Zhong, M. Skyllas-Kazacos, *J. Power Sources*, 39 (1992) 1
17. Wang WH, Wang XD. *Electrochim. Acta*, 24 (2007) 6755
18. Meyers JP, Doyle M, Darling RM, Newman, *J. Electrochem Soc*, 8 (2000) 2930
19. Albery WJ, Mount AR. *J. Electroanal Chem*, 325 (1992) 95
20. Xiao P, Gao WY, Qiu XP, Zhu WT, Sun J, Chen LQ, *J. Power Sources*, 182 (2008) 377
21. Oriji G, Katayama Y, Miura T, *Electrochim. Acta*, 49 (2004) 3091
22. W.H. Wang, X.D. Wang, *Electrochim. Acta*, 52 (2007) 6755